THE JOURNAL OF BIOLOGICAL CHEMISTRY VOL. 281, NO. 4, pp. 2380–2389, January 27, 2006

Analysis of NOD2-mediated Proteome Response to Muramyl Dipeptide in HEK293 Cells*[S]

Received for publication, June 1, 2005, and in revised form, October 18, 2005 Published, JBC Papers in Press, October 28, 2005, DOI 10.1074/jbc.M505986200

Dieter Weichart[‡], Johan Gobom[‡], Sina Klopfleisch[§], Robert Häsler[§], Niklas Gustavsson[‡], Susanne Billmann[§], Hans Lehrach[‡], Dirk Seegert[¶], Stefan Schreiber[§1], and Philip Rosenstiel[§]

From the [‡]Max Planck Institute of Molecular Genetics, D-14195 Berlin-Dahlem, [§]Institute of Clinical Molecular Biology, University Hospital Schleswig-Holstein, D-24105 Kiel, and [¶]Conaris Research Institute AG, D-24105 Kiel, Germany

NOD2, a cytosolic receptor for the bacterial proteoglycan fragment muramyl dipeptide (MDP), plays an important role in the recognition of intracellular pathogens. Variants in the bacterial sensor domain of NOD2 are genetically associated with an increased risk for the development of Crohn disease, a human chronic inflammatory bowel disease. In the present study, global protein expression changes after MDP stimulation were analyzed by two-dimensional PAGE of total protein extracts of human cultured cells stably transfected with expression constructs encoding for wild type NOD2 ($NOD2^{WT}$) or the disease-associated NOD2 L1007fsinsC ($NOD2^{SNP13}$) variant. Differentially regulated proteins were identified by matrix-assisted laser desorption ionization time-of-flight (MALDI-TOF) mass spectrometry (MS) peptide mass fingerprinting and MALDI MS/MS. The limited overlap in the responses of the NOD2-overexpressing cell lines to MDP included a down-regulation of heat shock 70-kDa protein 4. A complex pro-inflammatory program regulated by $NOD2^{WT}$ that encompasses a regulation of key genes involved in protein folding, DNA repair, cellular redox homeostasis, and metabolism was observed both under normal growth conditions and after stimulation with MDP. By using the comparison of $NOD2^{WT}$ and disease-associated $NOD2^{SNP13}$ variant, we have identified a proteomic signature pattern that may further our understanding of the influence of genetic variations in the *NOD2* gene in the pathophysiology of chronic inflammatory bowel disease.

NOD2 belongs to a growing family of regulatory nucleotide-binding oligomerization domain proteins with a central nucleotide-binding oligomerization domain and N-terminal caspase recruitment domains that are involved in programmed cell death and immune responses. The domain structure consists of two adjacent N-terminal caspase recruitment domains, a central nucleotide binding domain, and 10 C-terminal leucine-rich repeats (1). The leucine-rich repeats of NOD2 are homologous to those seen in R proteins and Toll-like receptors, which recognize pathogen-associated molecular patterns, thus enabling an innate cellular response to pathogens. Muramyl dipeptide (MurNAc-L-Ala-D-iso-Gln, MDP-LD)[2] derived from peptidoglycan was recently identified as the ligand of NOD2 (2, 3). Upon MDP stimulation, NOD2 has been shown to activate the transcription factor nuclear factor κB (NF-κB) by interacting with the RIP-like interacting CLARP kinase (RICK/RIP2) (4).

A frameshift mutation in the leucine-rich repeats of NOD2 (L1007fsinsC, SNP13), which leads to a partial truncation of the leucine-rich repeats in the protein, has been associated with the development of Crohn disease, a human chronic relapsing-remitting inflammatory bowel disease (5–7). The truncation leads to a decreased MDP responsiveness and subsequent NF-κB activation. Expression of NOD2 sensitizes intestinal epithelial cells to release the chemotactic cytokine IL-8 upon stimulation with bacterial cell wall components (8, 9). It has been shown recently that tumor necrosis factor-α up-regulates NOD2 in intestinal epithelial cells via an NF-κB-dependent mechanism (8–10). $Nod2^{-/-}$ mice are deficient in epithelial cryptdin expression and exhibit a higher susceptibility to oral *Listeria* infection (11). Thus, NOD2 has been implicated as a sentinel in maintaining the integrity of the intestinal barrier against luminal pathogens (12). However, the complex changes in protein expression subsequent to an activation of NF-κB induced by NOD2 remain to be elucidated.

We have addressed this task using a global proteomic approach. HEK293 cells were stably transfected with expression constructs encoding for the wild type form of NOD2 ($NOD2^{WT}$) or the disease-associated NOD2 L1007fsinsC variant ($NOD2^{SNP13}$) stimulated with MDP-LD for 4 and 24 h, respectively, and protein extracts were analyzed by two-dimensional GE. Differentially regulated protein spots were detected by a semi-automated digital image analysis system, sampled from the gel, and the contained proteins subsequently were identified by MALDI-TOF peptide mass fingerprinting and MALDI-TOF/TOF fragment ion analysis. Results for selected proteins were independently confirmed by immunoblots.

The identified proteins were categorized into functional groups, and their implications for pathophysiology of Crohn disease are discussed.

MATERIALS AND METHODS

Cell Culture and Generation of Stable Transfectants—Human HEK293 and myelomonocytic THP-1 cells were purchased from the German Collection of Microorganisms and Cell Cultures (Braunschweig, Germany). The cells were cultured in RPMI + 10% fetal calf serum. One day before transfection, the cells were seeded at a density of

* This work was supported by Deutsche Forschungsgemeinschaft Grant SFB 415, by the Proteomverbund Competence Network within the National Genome Research Network, the German Ministry for Education and Research, and the European Commission (EU FP5 Genomics of IBD). The costs of publication of this article were defrayed in part by the payment of page charges. This article must therefore be hereby marked "*advertisement*" in accordance with 18 U.S.C. Section 1734 solely to indicate this fact.

[S] The on-line version of this article (available at http://www.jbc.org) contains Figs. S1–S4 and Table 1.

[1] To whom correspondence should be addressed: Institute of Clinical Molecular Biology of the University Hospital Schleswig-Holstein, Campus Kiel, Schittenhelmstr. 12, D-24105 Kiel, Germany. Tel.: 49-431-597-1373; Fax: 49-431-597-1842; E-mail: s.schreiber@mucosa.de.

[2] The abbreviations used are: MDP-LD, MurNAc-L-Ala-D-iso-Gln; MDP-DD, MurNAc-D-Ala-D-iso-Gln; MDP, muramyl dipeptide; MALDI-TOF, matrix-assisted laser desorption ionization time-of-flight; MS, mass spectrometry; CHAPS, 3-[(3-cholamidopropyl)dimethylammonio]-1-propanesulfonic acid; PAF, platelet-activating factor; PAFAH, PAF acetylhydrolase; IL, interleukin; RT, reverse transcription; GE, gel electrophoresis; MTP, microtiter plate; siRNA, small interfering RNA; TEMED, *N*,*N*,*N*′,*N*′-tetramethylethylenediamine; F, forward; R, reverse.

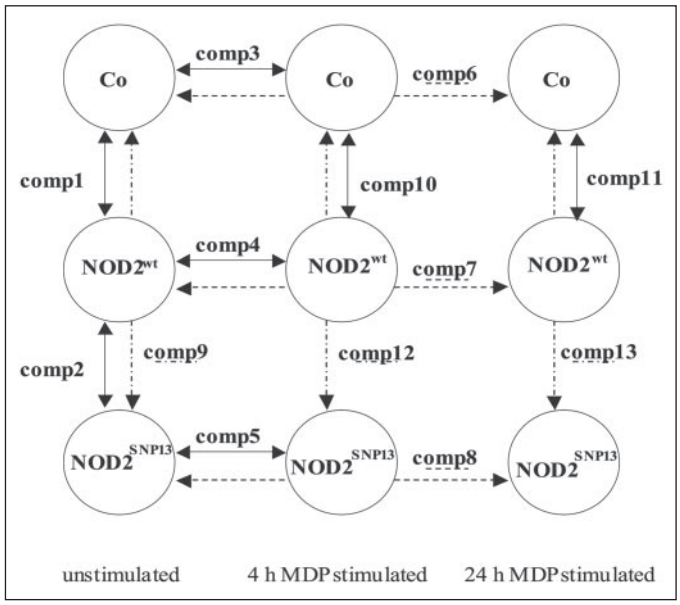

FIGURE 1. **Schematic representation of the experimental approach.** All comparisons considered in this study are depicted by *arrows*. The samples designated *Co* are from the control HEK293 cell line (mock-transfected); the $NOD2^{WT}$ samples are from the HEK293 cell line stably overexpressing the $NOD2^{WT}$ protein, and the $NOD2^{SNP13}$ samples are from the HEK293 cell line with a stable overexpression of the $NOD2^{SNP13}$ variant. The comparisons evaluated in this study are designated *comp1* to *comp13*. Each group represents five independent experiments depicted on individual gels.

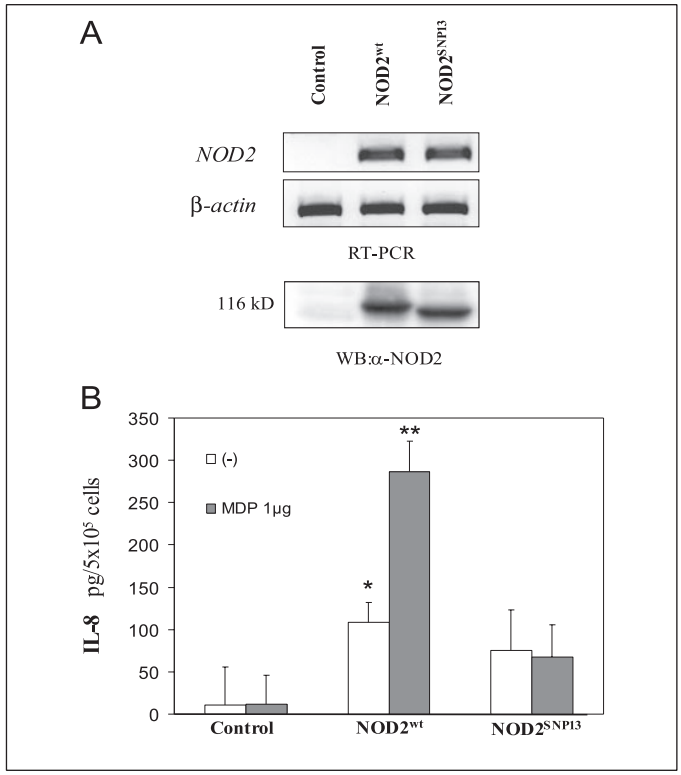

FIGURE 2. **Characterization of the stable HEK293 cell lines.** After selection and verification of protein expression, six independent stable clones were pooled per plasmid to generate polyclonal cell lines in order to avoid experimental bias from stable plasmid integration. *A* depicts expression of $NOD2^{WT}$ and $NOD2^{SNP13}$ on the mRNA (RT-PCR) and protein level (Western blot (*WB*)). The function of the stably expressed NOD2 protein was assessed by using an IL-8 enzyme-linked immunosorbent assay, which demonstrated a significant up-regulation of IL-8 secretion upon MDP stimulation (1 μg/ml) only in the $NOD2^{WT}$-transfected cells. The results are expressed as picograms of cytokine/5×10^5 cells (*B*). ($n = 3$ independent experiments in duplicate. *, $p < 0.05$; **, $p < 0.01$).

5×10^5 cells/2 ml on 6-well plates. Transfections were performed with FuGENE 6™ (Roche Applied Science) according to the manufacturer's manual, using 1 μg of the indicated plasmid/well. 48 h after the transfection, cells were selected over 4 weeks with 800 μg/ml G418 (Invitrogen) to select for stable transfectants. For each plasmid, 24 colonies were picked, after they had reached a diameter of 1 cm, and were assessed for stable expression of the encoded protein by Western blot. To avoid experimental bias from stable plasmid integration, six independent stable clones were pooled per plasmid to generate polyclonal cell lines. For confirmatory experiments, $NOD2^{WT}$- and $NOD2^{SNP13}$-expressing cells were generated with the FLP-IN system (Invitrogen). HEK293 cells containing the FRT recombination site were purchased from Invitrogen. Wild type and mutated (SNP13) NOD2 were inserted to the genomic recombination site by FLP recombinase enzyme. A control cell line was generated by transfecting an empty mock vector. All stable cell lines were selected for hygromycin B resistance and consequently cultured in Dulbecco's modified Eagle's medium + 10% fetal calf serum + 1% penicillin/streptomycin + 50 μg/ml hygromycin B (Invitrogen). Single colonies were picked and expanded in selection medium. Vector inserts and the genomic DNA context in the selected clones were sequenced to verify the NOD2 sequence and proper integration in the genomic locus.

Expression of NOD2 (wild type and SNP13) was monitored by immunoblotting using anti-NOD2 (Cayman Chemicals, Ann Arbor, MI) antibody. MDP-LD and MurNAc-D-Ala-D-iso-Gln (MDP-DD) were obtained from Bachem (Bubendorf, Switzerland) and applied at a concentration of 1 μg/ml.

IL-8 Enzyme-linked Immunosorbent Assay—Supernatants of HEK cell lines stimulated with MDP-LD were collected after 12 h. IL-8 was measured by enzyme-linked immunosorbent assay (R & D Systems, Minneapolis, MN) according to the manufacturer's protocol. The results were expressed as picograms of cytokine/5×10^5 cells.

Plasmid Constructs—The whole reading frame of NOD2 was amplified from pooled leukocyte cDNAs (MTC panel, Clontech) and cloned into the pcDNA3.1 vector (Invitrogen). The plasmid carrying the L1007fsinsC mutation (SNP13) was generated using a site-directed mutagenesis kit (Stratagene, La Jolla, CA). All constructs were sequence-verified using an ABI3700 sequencer (Applied Biosystems, Foster City, CA) prior to use. All primers were purchased from Eurogentec (Liège, Belgium).

Protein Extraction—From five parallel cell cultures for each cell line, the cells were harvested by centrifugation, and the pellets were weighed. Proteins were extracted from the pellets using a modification of the protocol of Klose and Kobalz (13). In short, the cells were ground in a ceramics mortar cooled in a liquid nitrogen bath, adding the 1.25-fold weight of a buffer containing 50 mM Tris (pH 7.1), 20% (v/v) glycerol (Sigma), and a protease inhibitor mixture (Complete™, Roche Applied Science). After 5 min of grinding under continued cooling, the homogenates were transferred to fresh vials where they were mixed with urea and thiourea in the ratio 3:2:1 (w/w) under continuous stirring at room temperature for 5 min. After the urea had dissolved, dithiothreitol (700 mM) was added to a final concentration of 70 mM, and the samples were stirred for another 25 min at room temperature. After removal of cell debris by centrifugation at 15,000 $\times$ *g* for 15 min at room temperature, the supernatants were stored at −80 °C until analysis by two-dimensional GE.

Two-dimensional Gel Electrophoresis—Isoelectric focusing was performed with an Ettan IPGphor™ apparatus (Amersham Biosciences) in 24-cm-long IPG strips with nonlinear gradients in the pH range of 3–10 (Amersham Biosciences). Prior to loading, the samples were centrifuged sharply for 30 min (22,000 $\times$ *g*; 25 °C) to remove insoluble aggregates and large organelles. Protein concentrations in the supernatant samples were determined with the two-dimensional Quant kit (Amersham Bio-

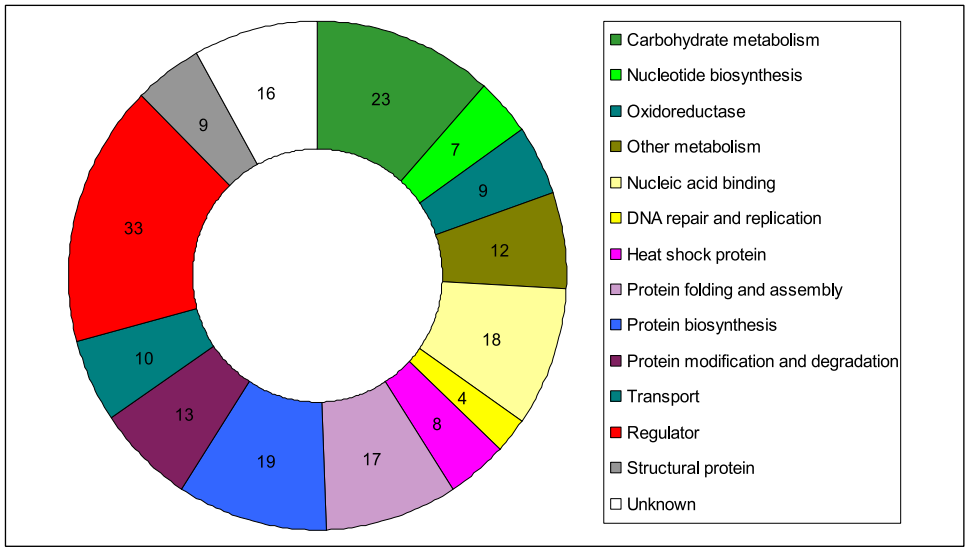

FIGURE 3. **Functional analysis ("clustering") of the 198 proteins identified in this study.** Numbers of proteins belonging to the functional classes are shown in the individual doughnut segments. For details of functional clustering, see "Results."

sciences). Samples containing 200 μg of protein were diluted to a final volume of 450 μl in a rehydration buffer consisting of 5 M urea (Merck), 2 M thiourea (Sigma), 2% CHAPS, 0.002% bromphenol blue, 0.8% IPG Buffer (pH 3–10) (Amersham Biosciences), and 1 tablet of Complete-eMini^{TM} protease inhibitor mixture (Roche Applied Science) per 1.5 ml.

For reduction and alkylation of cysteines, a one-step method using dithiodiethanol was employed (14). Dithiodiethanol (Fluka, Germany) was added 20 min prior to starting the isoelectric focusing to a final concentration of 100 mM.

The samples were loaded on the IPG strips by rehydration loading, and focusing was performed for 3 h at 30 V, followed by 6.5 h at 60 V. Subsequently, the voltage was increased to 500 V in a gradient over 1 h, and this voltage was maintained for another hour and thereafter increased first to 1000 V and then to 8000 V by a two-step gradient (1 h each). The final voltage of 8000 V was kept for another 7.5 h, providing a total of 60,000 V $\times$ h during the 21 h of focusing. After isoelectric focusing, the IPG strips were stored at -80 °C until further use.

For second dimension electrophoresis, standard continuous SDS-polyacrylamide gels were cast in Ettan DALT*twelve*^{TM} glass cassettes of 255 $\times$ 205 $\times$ 1 mm (Amersham Biosciences) with a final concentration of acrylamide of 12% (w/v). The acrylamide was obtained as ready (37.5:1) stock solution with 30% (w/v) (Biosolve BV, Valkenswaard, The Netherlands). Gel solutions were prepared with MilliQ water, filtered through 0.45-μm diameter cellulose acetate filters (Corning, NY), and degassed for 10 min before adding UltraPure^{TM} TEMED (Invitrogen) and ammonium peroxodisulfate (Merck). Gels were allowed to polymerize for 3 h at room temperature and for an additional 4–6 days at 5 °C before use.

Before loading onto SDS-polyacrylamide gels, the IPG strips were equilibrated for 30 min at room temperature with gentle agitation in a solution containing 100 mM dithiodiethanol, 2% (w/v) SDS, 6 M urea, 50 mM Tris-HCl (pH 8.8) and 30% (v/v) glycerol. Second dimension electrophoresis was performed in an ETTAN DALT*twelve*^{TM} chamber (Amersham Biosciences) following the manufacturer's instructions. When the running fronts were 2 or 3 mm from the lower end of the gel sandwich, the gels were fixed and stained. Colloidal Coomassie staining was performed according to the protocol by Doherty *et al.* (15). After staining, the two-dimensional gels were rinsed twice with MilliQ water and scanned with an EPSON 1640 XL A3 scanner in the transparency mode (8-bit gray scale).

Two-dimensional GE Image Analysis—The gel images were analyzed with the Proteomweaver 2.1 software (Definiens, Germany). After optimization of parameters, spot detection was performed with the following parameters: radius limit of 4, intensity limit of 2,000, and contrast limit of 10. This resulted in detection of 1,450–2,243 spots per gel, with an average of 1,960 spots per gel (from 9 randomly chosen gels). Based on the total protein load, it was estimated that 15–30 ng of protein could be detected reproducibly in one spot. The dynamic range exceeded 173, covering at least a range of 0.015–2.6 μg of protein per spot, corresponding to 0.0075–1.3% of the total protein loaded on the gel. Saturation of staining was not observed, as judged by the optical density distributions of the most dense protein spots. Automatic matching of spots was performed using Proteomweaver with maximum y/x shifts of 800 pixels, a pattern radius of 500 pixels, and a pattern size of 50 pixels. In a number of cases, spot editing and manual matching were required. Following the matching process, pair-match based normalization of data were performed with the Proteomweaver software. First a normalization factor was calculated for each pair of gels as the median of the quotients of the intensities of all matched spots, and from these an intensity factor was computed for each gel, allowing normalization of intensity data.

A reliable detection of regulation factors of 1.49 (single-sided regulation) was determined to be possible, if the data from the 500 most intense spots of 9 random pairs of gels were considered (with $p < 0.05$, from groups comprising 5 gels each). When drawing on the data from the 900 most intense spots, the reliable regulation factor was calculated to be 1.67 ($p < 0.05$). Consequently, for detection of protein spots with significant up- or down-regulation in any of the comparisons between cell lines or treatments, the minimal regulation factors were set to 1.5 and 0.667, respectively. This requirement was combined with the following settings. First, the gel spot must be detected in at least 4 of 5 gels in one group. Second, the mean intensity in that group was required to be at least 0.05 (arbitrary intensity units). Third, the Student's t test ($p < 0.05$) was used to filter out statistically insignificant variations in spot densities. It may be pointed out that the average intensities provided by the Proteomweaver software are geometric averages, not arithmetic averages. Clustering analysis and heat maps of differentially regulated proteins were generated using Spotfire Decisionsite 7.2 software (Spotfire, Somerville, MA).

Excision and Tryptic Digests of Protein Spots—For handling excised protein spots, 96-well polypropylene microtiter plates (MTPs) (Costar Thermowell, Cornis, NY) were used, and they were pierced in order to allow removal of solutions and recovery of protein digests. The protein

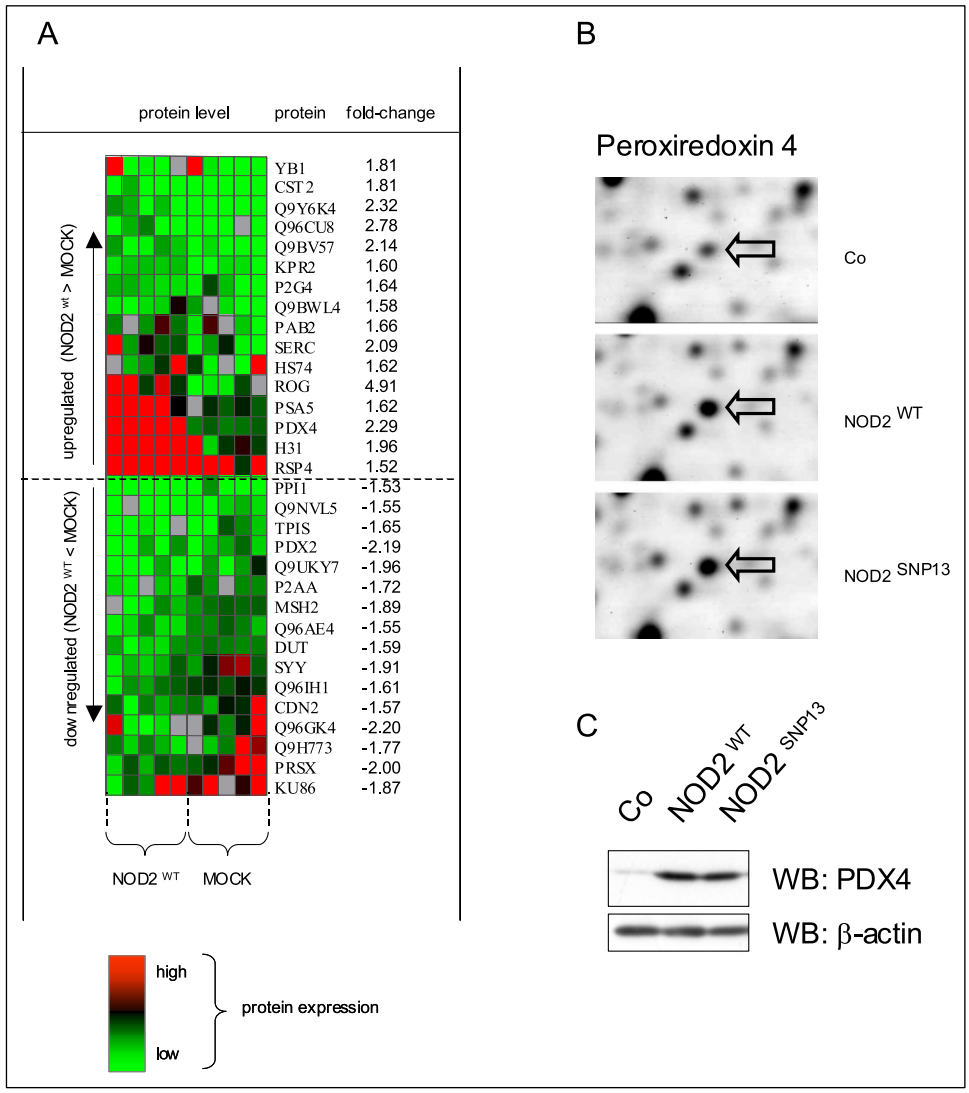

FIGURE 4. **Heat map of differentially expressed proteins in unstimulated HEK293 cells with stable expression of the wild type NOD2 protein compared with the control cell population.** *A*, the spot alignment and intensity was calculated using the Proteomweaver® program. A minimal regulation of ±1.5-fold combined with the following requirements was considered significant. (i) 4 of 5 gels in one group were required to have a detectable spot. (ii) The mean intensity in that group was required to be at least 0.05 (arbitrary intensity units). (iii) Student's *t* test value had to be $p < 0.05$. Each column represents a single independent experiment. *Gray boxes* show spots that could not be identified on the respective gel. *B*, regulation of the peroxiredoxin IV (PDX4) protein (encoded by *PRDX4*) in unstimulated cells. Averaged images from five two-dimensional gels each; *top*, mock-transfected (control, *Co*); *middle*, $Nod2^{WT}$-transfected; *bottom*, $Nod2^{SNP13}$-transfected. *C* shows an independent Western blot (*WB*) verification.

spots were excised from the two-dimensional gel at an automatic gel excision work station (Proteineer SP, Bruker Daltonics, Bremen, Germany) by using an excision tool with a diameter of 1.5 mm. The gel samples containing the protein spots were delivered into the wells of the modified MTPs. *In situ* tryptic digestion was performed according to Shevchenko *et al.* (16) with some modifications. First, the excised gel plugs were washed three times for 20 min in 100 μl each of washing buffer (50 mM NH_4CO_3 (pH 8), 50% (v/v) ethanol) and then dehydrated for 5 min with 100 μl of ethanol. Removal of buffers and ethanol between incubation steps was performed by centrifugation of the gel-containing MTPs for 1 min at 1000 × *g*. The gel pieces were then placed for 15 min in a vacuum centrifuge (Savant, SVC100H) in order to completely remove any remaining liquid. For digestion of proteins, a trypsin solution (Roche Applied Science) containing 10 ng/μl trypsin in 50 mM NH_4CO_3 (pH 8) was freshly prepared and kept on ice. 4 μl (40 ng of trypsin) of the trypsin solution was added to each gel piece, and these were incubated for 30 min at 4 °C. Subsequently, 8-μl volumes of 50 mM NH_4CO_3 (pH 8) buffer were added to each sample, and the digestion was performed at 37 °C for 4 h. The digestion was stopped by addition of 10 μl of extraction buffer containing 0.5% trifluoroacetic acid and 2 mM *n*-octyl glycopyranoside. The extracted peptides were recovered by centrifugation into fresh MTPs placed under the modified plates.

Mass Spectrometry—MALDI sample preparation was performed on MALDI 600–384 AnchorChip sample plates (Bruker Daltonics, Bremen, Germany) as described previously (17, 18). A TeMO automatic liquid handler (Tecan, Switzerland) was used to deposit 1-μl aliquots of the tryptic digests onto pre-formed microcrystalline layers of the MALDI matrix α-cyano-4-hydroxycinnamic acid. After the solvent had evaporated, the samples were briefly washed with 0.1% trifluoroacetic acid. Mass spectra of positive ions in the *m/z* range 640–4,000 were recorded on an Ultraflex LIFT and a Reflex III MALDI-TOF mass spectrometer (Bruker Daltonics, Bremen, Germany) operated in the reflector mode using delayed ion extraction. Fragment ion mass spectra of selected peptides, recorded on the MALDI-TOF/TOF instrument, were used for verification of uncertain identification results.

Selection of the first monoisotopic signals in the spectra was performed using the signal detection algorithm SNAP implemented in the FlexAnalysis software (Bruker Daltonics, Bremen, Germany). The spectra were calibrated using a recently described procedure (19) based on a combination of external calibration (using polyethanolglycol) followed by internal calibration using signals from tryptic autodigestion products (monoisotopic masses (MH^+) are as follows: 842.51, 1045.562, and 2211.1045 Da) and two peptide standards (human angiotensin I and human ACTH-(18–39); 1296.6853 and 2465.1989 Da, respectively).

The calibrated mass lists were then filtered, removing calibration masses and common contaminants. Protein identification was performed with the MASCOT data base search engine (version 1.8) querying primarily the SwissProt data base (SwissProt www.expasy.org/sprot/) and secondarily the NCBI data base (www.ncbi.nlm.nih.gov/). The minimum MOWSE scores used as requirement for identification were 52 for SwissProt searches (setting for organism *Homo sapiens*) and 66 for NCBI (setting for organism mammalia), corresponding to a statistical significance level of $p < 0.005$ in both searches. The identification of a protein was considered reliable if it was identified with this level of significance from at least two gels (without conflicting identifications in any parallel gels).

SDS-PAGE and Immunoblotting—Western blotting was performed as described (9). 15 μg of protein extract was separated by denaturing SDS-PAGE and transferred onto polyvinylidene difluoride membranes (Millipore, Billerica, MA). After blocking, the membranes were probed with specific primary antibodies, washed, and incubated with horseradish peroxidase-conjugated IgG as secondary antibody. The PDX2 and PDX4 antibodies were purchased from ACRIS (Littleton, CO), TCP-η from Santa Cruz Biotechnology (Santa Cruz, CA), and YB1 from Abcam (Cambridge, MA). The detected proteins were visualized by chemiluminescence (ECL, Amersham Biosciences).

siRNA Transfection and Luciferase Assay—Stable FLP-IN HEK293 cells were transfected with siRNAs against PDX4 (Invitrogen Stealth select HSS116212 and HSS116213) or a scrambled control without any homology to known transcripts together with 400 ng of NF-κB reporter plasmid and 100 ng of pRL-TK *Renilla* reference plasmid by using a standard protocol. 8 h later, transfection medium was replaced with regular cell culture medium. After 24 h MDP was added at the indicated concentration. Luciferase activity was determined after 8 h with a dual luciferase reporter gene kit from Promega according to the manufacturer's manual. The cells lysates were analyzed with a MicroLumatPlus LB96V microplate luminometer (EG & G Berthold, Wellesley, MA) after automatic injection of the necessary substrate solutions. All samples were at least measured in quadruplicates in three independent experiments. The results for firefly luciferase activity were normalized to *Renilla* luciferase activity.

RNA Isolation and RT-PCR—Total RNA was isolated using the RNeasy kit from Qiagen. 500 ng of total RNA were reverse-transcribed as described elsewhere (20). Primers used were as follows: NOD2_F, CGT TCT GCA CAA GGC CTA CC, and NOD2_R, TCC ATT CGC TTT CAC CGT G; PDX4_F, CAG CTG TGA TCG ATG GAG AA, and PDX4_R, ATC CTT ATT GGC CCA AGT CC; PDX2_F, GTG TCC TTC GCC AGA TCA CT, and PDX2_R, TGG GCT TAA TCG TGT CAC TG; TCPH_F, CCG AGC AGT TTA TGG AGG AG, and TCPH_R, CAA AGC CAG CAT TGT CAC AC; YB1_F, TGG GCG TCG ACC ACA GTA TT, and YB1_R, GCT GCT GAC CTT GGG TCT CA. For PCR, denaturation was for 5 min at 95 °C; 28 cycles of 30 s at 95 °C, 20 s at 58 °C, 60 s at 72 °C; final extension was for 5 min at 72 °C. To confirm the use of equal amounts of RNA in each experiment, all samples were checked in parallel for β-actin mRNA expression. All amplified DNA fragments were analyzed on 1% agarose gels and subsequently documented by a BioDoc Analyzer (Biometra, Göttingen, Germany).

RESULTS AND DISCUSSION

This study presents for the first time an analysis of the changes in the cellular proteome upon activation of NOD2 by using its ligand, the bacterial cell wall component MDP-LD, as a stimulus. The experimental design is schematically depicted in Fig. 1. The following three stable transfectants of HEK293 cells were used in the study: cells stably overexpressing NOD2^{WT}, cells overexpressing the mutant NOD2^{SNP13}, and mock transfected control cells (mock transfectant) (Fig. 2*A*). Samples were harvested from five parallel cell cultures under normal growth conditions and 4 and 24 h after the stimulation of the cells by MDP. Protein extracts were analyzed by two-dimensional GE. Transfected HEK293 cells represent an accepted model system for exploration of NOD2 signaling pathways, as the cells normally do not express NOD2 at detectable levels (1) (Fig. 2). The use of polyclonal cell lines excludes the risk of experimental bias from the stochastic chromosomal integration of the respective plasmids. The function of the stably expressed NOD2 protein was assessed using IL-8 enzyme-linked immunosorbent assay, which demonstrated a significant up-regulation of IL-8 secretion upon MDP stimulation (1 μg/ml) only in the NOD2^{WT} transfected cells (Fig. 2*B*).

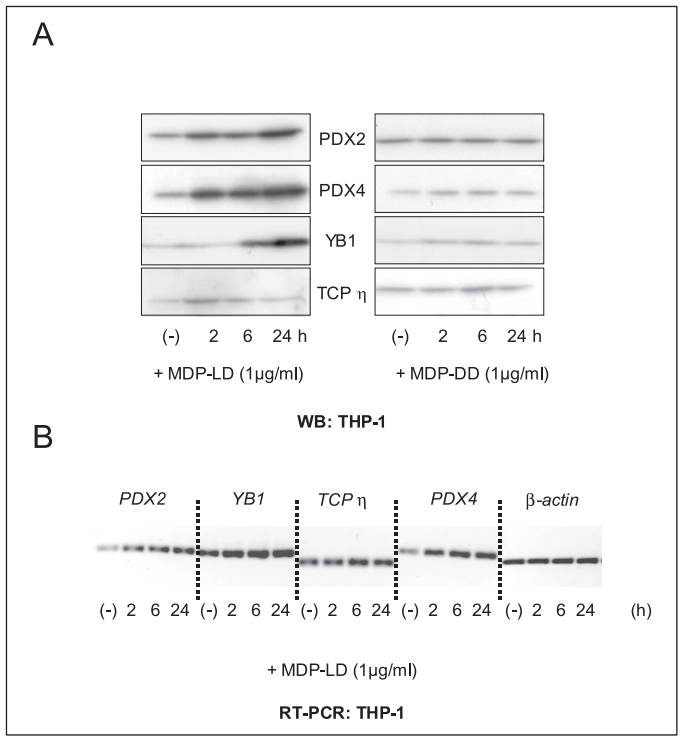

FIGURE 5. **NOD2-dependent regulation of selected proteins identified in the two-dimensional GE screen in THP1 myelomonocytic cells.** THP1 cells were stimulated with 1 μg/ml MDP-LD (active stereoisomer recognized by NOD2) or MDP-DD (inactive stereoisomer). At the indicated times, RNA and protein lysates were harvested. Protein lysates were subjected to Western blot analysis (*A*) with antibodies against PDX2, PDX4, YB1, and TTCPη. After isolation of total RNA, reverse transcription was performed, and *NOD2* target gene expression was assayed by semiquantitative RT-PCR to demonstrate whether the observed changes in the cellular proteome represent changes on the transcriptional level (*B*). Representative results of five independent experiments are shown.

Following spot detection and matching, each protein spot was assigned an identification number (SuperSpotID) by which it can be tracked on all gel images where it was detected. Normalization of protein staining intensities, as described above, allowed quantitative comparisons of protein abundance between any samples in the study.

In total, 198 protein species were identified that changed significantly in abundance by NOD2^{WT} or NOD2^{SNP13} overexpression and/or MDP stimulation. These proteins are listed in supplemental Table 1, including their averaged, normalized spot densities in the different analyses. The averaged gel images for each sample are shown in supplemental Fig. 1, annotated with SuperSpotIDs.

Classification of Regulated Proteins—The identified proteins were sorted into functional groups derived from information obtained from SwissProt/TrEMBL and, for proteins with no assigned function in those

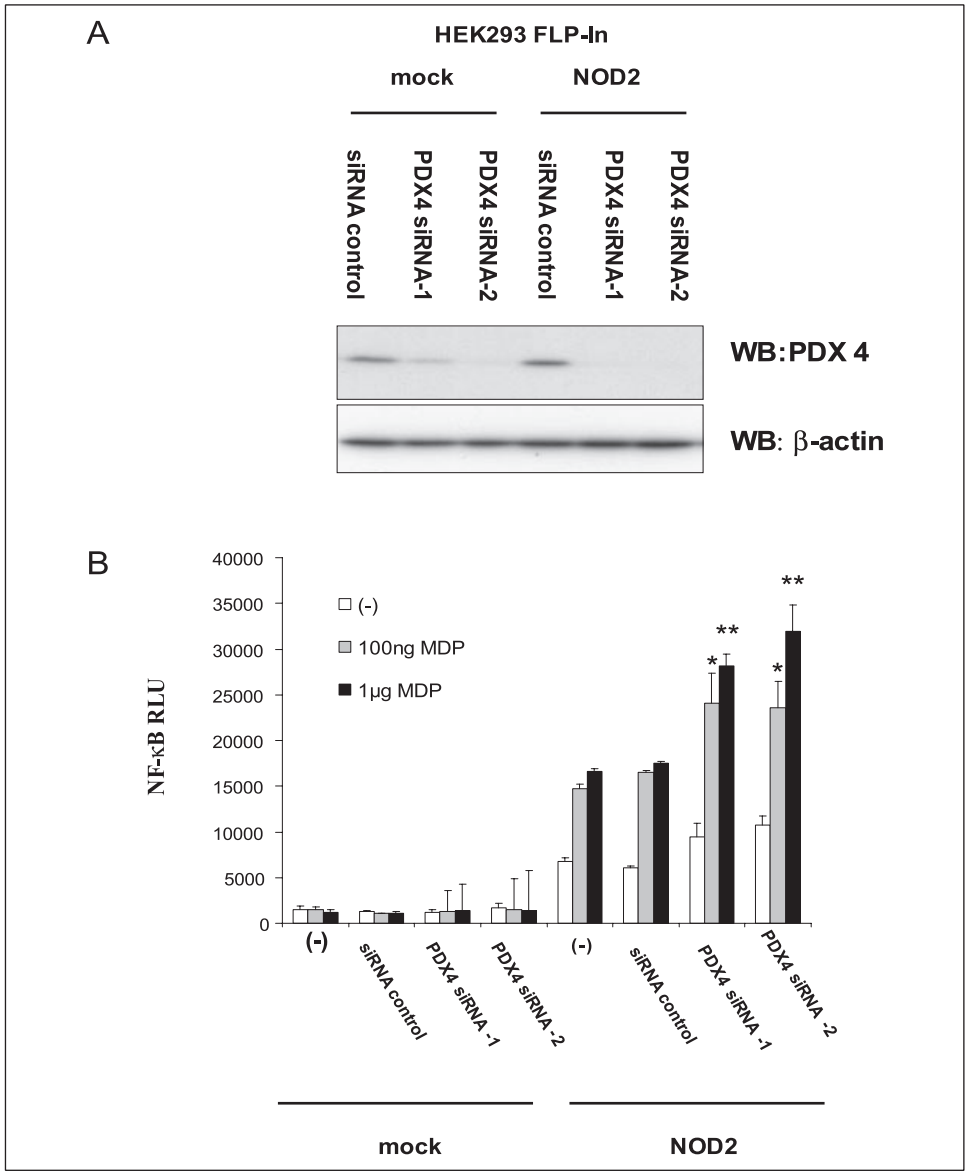

FIGURE 6. **Silencing of PDX4 enhances MDP-induced NF-κB activation in NOD2^{WT}-expressing cells.** *A,* Western blot (*WB*) analysis of stable FLP-In cells HEK293 cells with recombinase-based integration NOD2^{WT} or the empty vector cassette. Cells were transfected with two different siRNAs against PDX4 or a control siRNA in the presence of the reporter plasmids pNF-κB-Luc and pRL-TK as described (29). After 24 h, silencing of PDX4 was assessed using Western blot. Note that the FLP-IN cells carry a single copy of the NOD2 expression cassette. *B,* in parallel, identically treated cells were stimulated with the indicated doses of MDP for 8 h. Luciferase activity was determined by dual luciferase assay as described. Normalization regarding transfection efficiency was performed by concomitant measurement of *Renilla* luciferase activity. All samples were at least measured in quadruplicate in three independent experiments. Results are expressed in mean relative light units ± S.E.; *, $p < 0.05$; **, $p < 0.01$.

data bases, through InterPro searches (GO classification, www.ebi-.ac.uk/interpro/). In order for each protein to appear only in one category, the following hierarchy of protein functions was defined: regulator > DNA repair and replication > nucleic acid binding > protein folding and assembly > heat shock protein > protein modification and degradation > protein biosynthesis > nucleotide biosynthesis > carbohydrate metabolism > oxidoreductase > other metabolism > transport > structural protein > unknown function.

The result of this functional analysis is shown in Fig. 3. Of the 198 protein spots identified, 33 have been described in the literature as regulator proteins or putative regulator proteins; 22 were nucleic acid-binding proteins, DNA repair, or replication proteins (without proven involvement in any regulation); 32 proteins were involved in the biosynthesis, modification, or degradation of proteins; and 25 were heat shock proteins or involved in protein folding or assembly. Of the 16 protein spots containing proteins of unknown function, 10 were novel proteins without assigned functions so far (supplemental Table 1). The observed protein distributions resembles those reported in previous work on the general influences of muramyl dipeptide on DNA and protein synthesis (21–24).

As expected for proteomic studies, the functional distribution observed in this study is slightly skewed if compared with the molecular function data available for all human genes from EBI (www.ebi.ac.uk; 19,779 entries as of 14.01.2005). For example, according to EBI data, about 19.9% regulators (adding up the classes GO:0030528, GO:0030234 and GO:0004871) and 15.5% of genes with nucleic acid binding function would be expected, although in our study the corresponding numbers are 16.6 and 9%, respectively. This discrepancy can be explained with the existence of genes coding for regulatory and nucleic acid-binding RNAs and with the occurrence of tissue-specific and low level regulatory proteins, which are not normally detected on two-dimensional gels of whole-cell lysates. Proteins involved in metabolic processes are, on the other hand, over-represented, as would be expected because of their predominantly high cellular concentrations. The functional classes of transport and structural proteins are covered in this study with the frequency expected from genomic data (about 5% each).

Altered Protein Abundances in Unstimulated NOD2^{WT} and NOD2^{SNP13} Transfectants—Overall, 32 proteins were detected that differed in abundance between the unstimulated mock transfectants and the NOD2^{WT} (Fig. 1, *comp1*). The significantly regulated proteins are depicted in a heat map (Fig. 3*A*). That this number is relatively large may

TABLE 1

Influences of overexpressed NOD2 variants on protein expression changes

The regulation factors given are ratios of protein spots levels in unstimulated cells carrying $NOD2^{SNP13}$ divided by their levels in unstimulated cells carrying $NOD2^{WT}$.

SuperSpot ID	Protein name	Gene name	Protein description	Regulation factor
34291	MAT3	*MATR3*	Matrin 3	2,365
33385	TPIS[a]	*TPI1*	Triose-phosphate isomerase (TIM)	2,213
33569	PPI1	*PITPN*	Phosphatidylinositol transfer protein α isoform (PI-TP-α)	1,804
34061	ALFA	*ALDOA*	Fructose-bisphosphate aldolase A (lung cancer antigen NY-LU-1)	1,722
33588	Q96GK4	*MEP50*	Hypothetical protein MGC2722	1,667
33589	Q96IH1	*11148*	FSC1_HUMAN, Fascin 1, p55, 55-kDa actin-bundling protein	1,638
33538	PRSX	*PSMC6*	26 S protease regulatory subunit S10B (proteasome subunit p42)	1,629
34167	ROC	*HNRPC*	Heterogeneous nuclear ribonucleoproteins C1/C2	1,523
33379	SERA	*PHGDH*	D-3-phosphoglycerate dehydrogenase (3-PGDH)	0,651
33373	SERC	*PSAT1*	Phosphoserine aminotransferase (PSAT)	0,613
33683	PPCM	*8725*	Mitochondrial phosphoenolpyruvate carboxykinase (PEPCK-M)	0,579
34475	Q9NP82	*NT5C*	5′(3′)-Deoxyribonucleotidase, cytosolic type	0,570
33697	PD6I	*PDCD6IP*	Programmed cell death 6-interacting protein, HP95	0,512
33981	TERA	*VCP*	Transitional endoplasmic reticulum ATPase (TER ATPase) (VCP)	0,391
34080	Q9Y6K4	*PPP1R7*	Protein phosphatase-1 regulatory subunit 7α2	0,336

[a] TPIS indicates triose-phosphate isomerase.

be due to the fact that expression of NOD2 above physiological levels may activate downstream signaling pathways to a certain extent (1). The corresponding number for the comparison between the unstimulated mock transfectants and $NOD2^{SNP13}$ (Fig. 1, *comp*) is 20 proteins. Among these two sets, 9 proteins share a similar regulation, including nucleic acid-binding proteins ROG and H31, protein biosynthesis proteins SYY and RSP4, DNA repair protein MSH2, and peroxiredoxin 4 (PDX4). PDX4 has been implicated in the modulation of the NF-κB pathway (25), and its regulation in the two-dimensional GE (Fig. 2*B*) was verified by Western blot analysis (Fig. 4*C*). Parallel regulation in cell lines overexpressing $NOD2^{WT}$ and $NOD2^{SNP13}$ might reflect the conserved ability of $NOD2^{SNP13}$ to induce basal signaling upon overexpression despite a clear defect in MDP-induced NF-κB activation (26, 27). Most interestingly, we could confirm the NOD2-mediated PDX4 up-regulation in THP-1 cells, which express endogenous levels of NOD2 (28). Upon stimulation with the NOD2-ligand MDP-LD, a prolonged PDX4 transcript and protein up-regulation were detectable by Western blot and RT-PCR (Fig. 5, *A* and *B*). To exclude an unspecific effect, the MDP-DD stereoisomer was employed, which is not recognized by NOD2 (2, 3). Stimulation with this compound did not result in a significant up-regulation of PDX4 (Fig. 5*A*).

We further investigated the putative influence of PDX4 on NOD2-induced signaling pathways. NF-κB activation after MDP stimulation was assessed in the isogenic stable HEK cell populations (FLP-IN). *PDX4* gene expression was silenced using two different siRNAs, which independently down-regulated PDX4 protein levels (Fig. 6*A*). A robust NF-κB activation after MDP stimulation (1 μg/ml) was seen exclusively in the $NOD2^{WT}$-transfected cells. The NF-κB transactivation was significantly enhanced by PDX4 knock down (Fig. 6*B*). Thus, the NOD2-mediated induction of PDX4 could be part of a negative feedback loop modulating NF-κB activation downstream of NOD2.

Comparison between unstimulated $NOD2^{WT}$ and $NOD2^{SNP13}$ cell lines (comp2) revealed several differentially expressed proteins (Table 1), including a regulatory subunit of protein phosphatase 1 (Q9Y6K4, see below), two proteasome complex proteins (PSA5 and PSE2), and cyclophilin A (PPIA) which is involved in protein folding.

These results emphasize the importance of the concept of the "basal activation" of NOD proteins, *i.e.* auto-activation by high expression levels (27). In the experimental system used for our initial screen, $NOD2^{WT}$ and $NOD2^{SNP13}$ are expressed at high levels. Proteins, which were identified to be differentially regulated by NOD2 expression in the absence of the NOD2-ligand, may be regulated in an MDP-dependent manner in other cell types expressing low endogenous levels of NOD2 (*e.g.* monocytes) as demonstrated for PDX4 (Fig. 5, *A* and *B*). However, NOD2 can be expressed in high levels (*e.g.* in intestinal epithelial cells under inflammatory conditions). Thus, it will be interesting to assess further the contribution of auto-activation for NOD2-induced signaling.

Time Course of MDP-induced Changes in Protein Abundance—The kinetics of proteome responses to MDP was assessed following 4 and 24 h of stimulation. The response of the three cell lines to MDP stimulation differed significantly. Fig. 7 shows the regulated proteins clustered according to their co-regulation among the three cell lines, after 4 and 24 h of MDP stimulation. As evident from Fig. 7 and Supplemental Fig. 3, a number of proteins exhibited transient regulation by MDP, as observed after 4 h of stimulation, although other proteins showed sustained regulation by MDP even after 24 h. For example, in the mock transfectant, permanent induction was detected for the putative protein phosphatase-1 regulatory subunit 7α2 (Q9Y6K4, encoded by the *PPP1R7* gene). This protein might be active in regulating phosphorylation events relevant to cell division (30). In unstimulated cells, the levels of Q9Y6K4 are also elevated in $NOD2^{WT}$, but not in $NOD2^{SNP13}$, if compared with levels in the control cell line.

Among the proteins regulated in a $NOD2^{WT}$-specific manner are the Crk-like protein and phosphoglycerate kinase 1 (PGK1). Crk-like protein is an oncogene and an adaptor protein involved in several signaling processes. It has been shown that it associates with WASP (31), ASAP1 (32), BCR-ABL (33, 34), DOCK2 (35), and STAT5 (36), among others. Furthermore, this protein provides a link between Jak kinases and downstream cascades that act in interferon-dependent transcriptional regulation (37). The PGK1 protein is an enzyme of the glycolytic pathway, but as a primer recognition protein it also modulates DNA replication and repair in mammalian cells (38, 39). PGK1 may also be secreted and participates in angiogenic processes as a disulfide reduc-

tase (40). Peroxiredoxin 2 (PDX2) was initially described as natural killer cell enhancing factor-B (41–44) and has been implicated as a cellular peroxidase that eliminates endogenous H_2O_2 produced in response to growth factors such as platelet-derived growth factor and epidermal growth factor (45). Y-box factor YB1 belongs to the highly conserved family of cold shock proteins, and YB1 appears to regulate gene expression interfering with p53 signaling (46–48). T-complex protein 1η (TCPH) belongs to the cytosolic chaperonin CCT complex, which has been shown to mediate the ATP-dependent folding of a set of proteins *in vivo,* including cytoskeletal protein and cyclin E (49, 50). Functional TCPH is required for cyclin E maturation and has been shown to be overexpressed in colonic adenocarcinoma suggesting that TCPH *in vivo* might be pivotal in maintaining the adequate protein machinery required for growth and proliferation in intestinal epithelial cells (49, 50).

The observed up-regulation of PDX2, YB1, and TCPH in the two-dimensional GE experiments was again confirmed in THP-1 cells differentially stimulated with MDP-LD and MDP-DD by Western blot analysis (Fig. 5*A*). Only endogenous NOD2 activation by MDP-LD led to a marked increase of PDX2, YB1, and TCPH protein levels, whereas the inactive stereoisomer MDP-DD had no effect. To establish whether the observed changes are caused by transcriptional activation or reflect post-transcriptional regulations, cDNA from stimulated THP-1 cells was amplified using specific primers for PDX2, PDX4, YB1, and TCPH. Here a clear increase of mRNA levels of PDX2 and PDX4 paralleling the protein up-regulation was observed, whereas only a moderate increase of TCPH and YB1 mRNA could be detected (Fig. 5*B*). Similar results were obtained using isogenic stable HEK293 cells (FLP-IN) carrying a single copy of $NOD2^{WT}$, $NOD2^{SNP13}$, or the empty vector cassette (supplemental Fig. S4).

The NOD2-dependent changes in protein abundance after MDP stimulation were further analyzed by comparing protein levels in $NOD2^{WT}$ with those in the mock transfectant after MDP stimulation (Fig. 1, *comp10* and *comp11*). Significant up-regulation of proteins by MDP in $NOD2^{WT}$ (relative to unstimulated cells, Fig. 1, *comp4* and *comp7*) concomitant with elevated levels of those proteins in the $NOD2^{WT}$ cell line (relative to the control) was detected for 8 protein spots. Down-regulation by MDP and by $NOD2^{WT}$ overexpression was observed for 4 protein spots (see supplemental Table 1). For interpretation of the data, it is important to examine whether the protein spots are isoforms that might be differentially regulated. In Table 2, the data are listed for those significantly regulated proteins that display only one isoform in our study and that are consequently amenable to interpretation. Only a single protein with regulation by MDP in the mock transfectant and with concomitant changes in $NOD2^{WT}$ was detected (namely, spot 33545, which is an isoform of β-actin).

The PSE1 protein (product of the gene *PSME1*) was observed at elevated levels throughout the experiments in $NOD2^{SNP13}$, relative to levels in the mock transfectant, although in $NOD2^{WT}$ it was elevated significantly only after 24 h of MDP stimulation. This protein, also known as REG-α or PA28a, is involved in immunoproteasome assembly and required for efficient antigen processing, and it has been reported to be up-regulated by interferon γ (51). Most interestingly, PSE2, another subunit of the PA28 activator complex, has also been identified in this study, but this protein shows different patterns of regulation.

From the presented data, it is clear that distinct effects of MDP exist in all three cell lines. Shared effects between groups, *e.g.* a down-regulation of the heat shock 70-kDa protein 4 (HS74) at 4 and 24 h in the $NOD2^{WT}$ and $NOD2^{SNP13}$ cell lines, point to common pathways that are responsible for the overlap. One possible explanation could be a

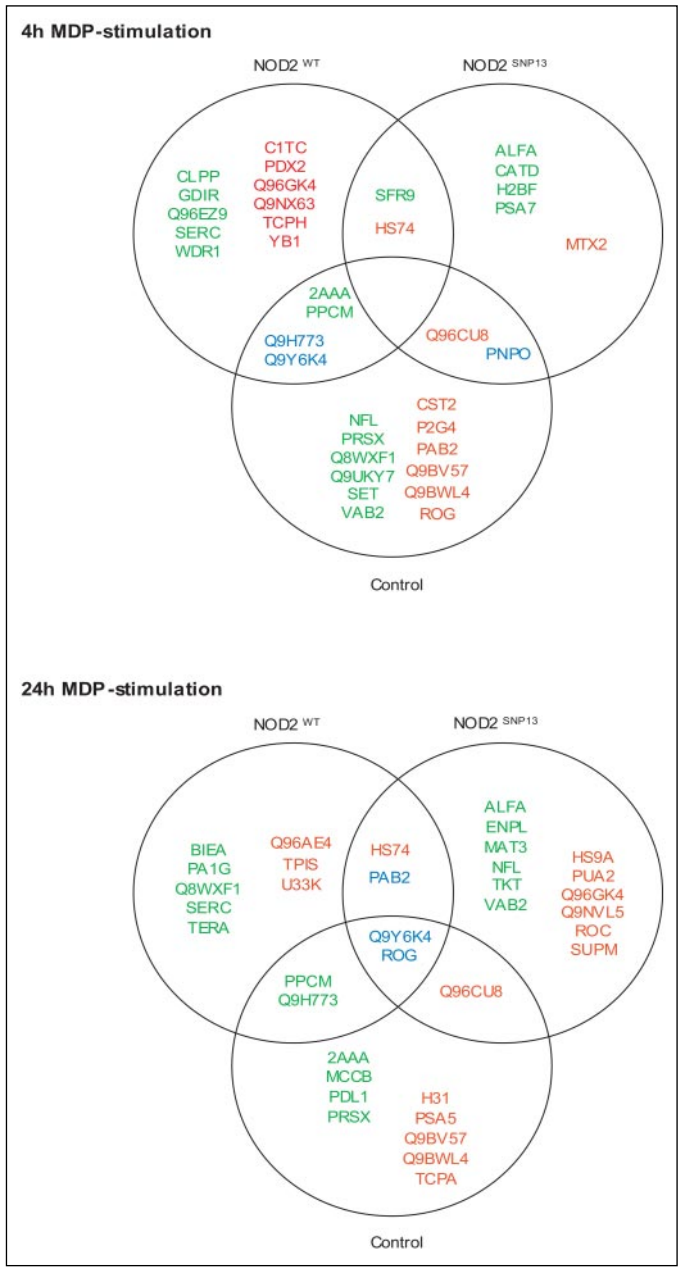

FIGURE 7. **Venn diagrams identify clusters of specifically regulated proteins upon MDP stimulation in each cell line.** Significantly regulated proteins in the three cell lines 4 and 24 h after MDP stimulation (relative to unstimulated cells) are illustrated in Venn diagrams to show common as well as group-specific responses. Up-regulated proteins are shown in *red*; down-regulated proteins are shown in *green*, and in the overlapping areas proteins regulated in opposing directions are shown in *blue*.

background expression of endogenous wild type NOD2. Although this possibility cannot be completely ruled out, several lines of evidence argue against this explanation as follows. (i) NOD2 mRNA and protein are not detectable in HEK293 cells (1). (ii) MDP activates canonical NF-κB signaling via NOD2, which is only observed in HEK293 cells stably or transiently transfected with NOD2 (1). (iii) There is a clear set of proteins that is specifically up-regulated in the $NOD2^{WT}$-transfected cells and cannot be found in any other group (Fig. 7).

MDP has also been described as the ligand for the inflammasome protein NALP3/CIAS1, which has been implicated in the generation of mature IL-1β (52). We detected neither NALP3 mRNA nor protein in our cell lines at any time point (data not shown), making it tempting to

TABLE 2

Selected examples of NOD2-dependent changes in protein abundance after MDP stimulation

Regulation by MDP was assessed in the NOD2^{WT}-overexpressing cell line, with regulation factors expressed relative to protein levels in unstimulated NOD2^{WT} cells (1st column, comp4 and comp7, respectively), whereas NOD2-dependent changes are expressed as ratios of NOD2^{WT} levels relative to levels in corresponding samples from the mock transfectant (2nd column, comp10 and comp11, respectively).

SuperSpot ID	Protein name	Gene name	Protein description	After MDP	MDP regulation (1)	WT to mock (2)
34116	Q9NX63	*CHCHD3*	Hypothetical protein FLJ20420	4 h	1.93	1.96
34204	H2BF	*HIST1H2BN*	Histone H2B.F (H2B/F)(H2B.1)	4 h	1.91	2.17
33858	PGK1	*PGK1*	Phosphoglycerate kinase 1 (PRP2)	24 h	1.57	1.59
33525	Q8WXF1	*PSPC1*	Paraspeckle protein 1	24 h	0.52	0.43
34081	PA1G	*PAFAH1B3*	Platelet-activating factor acetylhydrolase IB γ subunit	24 h	0.59	0.53

speculate that MDP exerts its common effects via NOD2/NALP3-independent mechanisms. A recent report has demonstrated that surface calreticulin can act as an alternate receptor for muramyl dipeptide and induces apoptotic signaling in RK13 cells (53, 54). In accordance to previous reports (1, 5), we did not detect significant cell death induced by MDP in HEK293 cells; however, the possibility of nonapoptotic signaling via calreticulin is under current investigation.

The significant regulation of proteins triggered by MDP stimulation in the NOD2^{SNP13} cells points to a signaling capacity of the truncated protein, which may be different from the NOD2^{WT} protein. In fact, we detected a cluster of proteins up-regulated by MDP stimulation in NOD2^{SNP13} cells, which were specific to this genetic variant. For example, MTX2 (metaxin 2), a mitochondrial membrane protein up-regulated in lipopolysaccharide-induced liver injury (55), was significantly up-regulated after 4 and 24 h. Similarly, transient down-regulation of cathepsin D was seen only in the NOD2^{SNP13} cells after 4 h. Cathepsin D is a major lysosomal protease mediating programmed cell death induced by interferon-γ, Fas/APO-1, and tumor necrosis factor-α (56). The observation of NOD2^{SNP13}-dependent regulation is in contrast to the established view that NOD2^{SNP13} is a loss of function mutation. In fact, a recent study also could demonstrate that macrophages from mice with a mutation corresponding to human NOD2^{SNP13} show increased mitogen-activated protein kinase activation and cytokine release upon MDP stimulation (57). Further studies will be required to molecularly dissect signaling downstream of activated NOD2^{SNP13}.

The only proteins described so far as being expressed NOD2-dependently are IL-8 (9) and IL-1β (58), and α-defensins (11, 59) were not detected in this analysis. The low abundance of these proteins might preclude monitoring the amounts of these proteins by two-dimensional GE because of the detection limit of the system, which is ~0.015 μg of protein per spot (corresponding to 0.0075% of total protein). Therefore, the presented proteome responses depict the changes only in medium to highly abundant protein species, although low expressed proteins may not be detected. Still, two-dimensional GE provides a powerful technology that has been used successfully to study altered protein expression patterns on a global level, for example in the identification of mitogen-activated protein kinase pathway signaling targets (60) or in deciphering the activation response of lipopolysaccharide-primed monocytes (61).

It should be mentioned that none of the regulated proteins detected in this study have been described as NF-κB target genes. Thus, the investigation of other signaling pathways, *e.g.* the activation of heat shock responsive elements, may lead to a novel understanding of NOD2-mediated signaling in intestinal disease.

Some of the regulated proteins emerging from our study have already been implicated in the pathophysiology of inflammatory bowel disease. For example, the down-regulation of tumor suppressor protein p16 (CDN2; INK4; gene product of *CDKN2A*) and mismatch repair gene *MSH2* have been implicated in inflammation-associated carcinogenesis (62–65).

The metabolic enzyme triose-phosphate isomerase (TPIS, Table 1) and the regulator proteins GDIR and PA1G have been described in the same type of regulation after stimulation of monocytes with lipopolysaccharide (61) as observed in our study after MDP stimulation. PA1G is the platelet-activating factor acetylhydrolase γ subunit (PAFAH 29-kDa subunit, also called PA1B3; gene product of *PAFAH1B3*) and is down-regulated in NOD2^{WT} cells upon 24 h of MDP treatment (Table 2). PAFAHs catalyze the removal of the acetyl group of the glycerol backbone of PAF, producing biologically inactive lyso-PAF. Most interestingly, PAF has been described as a potent and endogenous mediator in inflammatory intestinal processes, including inflammatory bowel disease. PAFAH activity is decreased in the ileal mucosa of patients with Crohn disease, and PAFAH activity in plasma of Crohn disease patients is inversely related to disease activity (66, 67). In addition, elevated levels of the "natural killer cell enhancing factor" peroxiredoxin 2 (NKEFB; PDX2) in cells carrying NOD2^{WT} is in accordance with the DNA microarray data reported for samples from patients with Crohn disease (68) and may define a pathway of clinical relevance.

The description of changes in proteomic patterns in the three different HEK293 cell lines gives several clues regarding the physiological cellular responses to the bacterial cell wall component MDP. (i) It defines a part of the complex pro-inflammatory program regulated by NOD2 that encompasses a regulation of key genes involved in protein folding, DNA repair, cellular redox homeostasis, and metabolism. On the other hand, NOD2-mediated up-regulation of peroxiredoxin 4 could serve as part of a negative feedback loop attenuating the NF-κB activation upon ligand recognition. (ii) It unveils a common response pattern to MDP, which includes the regulation of a protein phosphatase-1 subunit, indicating the existence of a general MDP sensor that is independent from NOD2 and NALP3. Although the observed changes describe alterations of abundant proteins in the cell, the results also describe the complexity and dynamics of the cellular proteome, which may not reflect simple pathways (*e.g.* NF-κB activation). (iii) The comparison of the programs initiated by wild type NOD2 and the mutated NOD2 form, which renders individuals susceptible for Crohn disease, may provide a signature pattern that could lead to a deeper understanding of the influence of defective NOD2 in the complex barrier dysfunction observed in chronic inflammatory bowel disease.

Acknowledgments—We are grateful to Patrick Giavalisco (Max Planck Institute, Berlin, Germany) and Axel Oberemm (BfR, Berlin, Germany) for help and advice concerning preparation of protein samples and two-dimensional gel separation. We also thank Tanja Kaacksteen and Ilka Ocker (Kiel, Germany) and Beata Lukaschewska and Dorothea Theiss (Max Planck Institute, Berlin, Germany) for their expert technical assistance.

REFERENCES

1. Ogura, Y., Inohara, N., Benito, A., Chen, F. F., Yamaoka, S., and Nunez, G. (2001) *J. Biol. Chem.* **276,** 4812–4818
2. Girardin, S. E., Boneca, I. G., Viala, J., Chamaillard, M., Labigne, A., Thomas, G., Philpott, D. J., and Sansonetti, P. J. (2003) *J. Biol. Chem.* **278,** 8869–8872
3. Inohara, N., Ogura, Y., Fontalba, A., Gutierrez, O., Pons, F., Crespo, J., Fukase, K., Inamura, S., Kusumoto, S., Hashimoto, M., Foster, S. J., Moran, A. P., Fernandez-Luna, J. L., and Nunez, G. (2003) *J. Biol. Chem.* **278,** 5509–5512
4. Inohara, N., Koseki, T., Lin, J., del Peso, L., Lucas, P. C., Chen, F. F., Ogura, Y., and Nunez, G. (2000) *J. Biol. Chem.* **275,** 27823–27831
5. Ogura, Y., Bonen, D. K., Inohara, N., Nicolae, D. L., Chen, F. F., Ramos, R., Britton, H., Moran, T., Karaliuskas, R., Duerr, R. H., Achkar, J. P., Brant, S. R., Bayless, T. M., Kirschner, B. S., Hanauer, S. B., Nunez, G., and Cho, J. H. (2001) *Nature* **411,** 603–606
6. Hugot, J. P., Chamaillard, M., Zouali, H., Lesage, S., Cezard, J. P., Belaiche, J., Almer, S., Tysk, C., O'Morain, C. A., Gassull, M., Binder, V., Finkel, Y., Cortot, A., Modigliani, R., Laurent-Puig, P., Gower-Rousseau, C., Macry, J., Colombel, J. F., Sahbatou, M., and Thomas, G. (2001) *Nature* **411,** 599–603
7. Hampe, J., Cuthbert, A., Croucher, P. J. P., Mirza, M. M., Mascheretti, S., Fisher, S., Frenzel, H., King, K., Hasselmeyer, A., MacPherson, A. J. S., Bridger, S., van Deventer, S., Forbes, A., Nikolaus, S., Lennard-Jones, J. E., Foelsch, U. R., Krawczak, M., Lewis, C., Schreiber, S., and Mathew, C. G. (2001) *Lancet* **357,** 1925–1928
8. Hisamatsu, T., Suzuki, M., Reinecker, H. C., Nadeau, W. J., McCormick, B. A., and Podolsky, D. K. (2003) *Gastroenterology* **124,** 993–1000
9. Rosenstiel, P., Fantini, M., Brautigam, K., Kuhbacher, T., Waetzig, G. H., Seegert, D., and Schreiber, S. (2003) *Gastroenterology* **124,** 1001–1009
10. Gutierrez, O., Pipaon, C., Inohara, N., Fontalba, A., Ogura, Y., Prosper, F., Nunez, G., and Fernandez-Luna, J. L. (2002) *J. Biol. Chem.* **277,** 41701–41705
11. Kobayashi, K. S., Chamaillard, M., Ogura, Y., Henegariu, O., Inohara, N., Nunez, G., and Flavell, R. A. (2005) *Science* **307,** 731–734
12. Schreiber, S., Rosenstiel, P., Albrecht, M., Hampe, J., and Krawczak, M. (2005) *Nat. Rev. Genet.* **6,** 376–388
13. Klose, J., and Kobalz, U. (1995) *Electrophoresis* **16,** 1034–1059
14. Olsson, I., Larsson, K., Palmgren, R., and Bjellqvist, B. (2002) *Proteomics* **2,** 1630–1632
15. Doherty, N. S., Littman, B. H., Reilly, K., Swindell, A. C., Buss, J. M., and Anderson, N. L. (1998) *Electrophoresis* **19,** 355–363
16. Shevchenko, A., Wilm, M., Vorm, O., and Mann, M. (1996) *Anal. Chem.* **68,** 850–858
17. Gobom, J., Schuerenberg, M., Mueller, M., Theiss, D., Lehrach, H., and Nordhoff, E. (2001) *Anal. Chem.* **73,** 434–438
18. Nordhoff, E., Egelhofer, V., Giavalisco, P., Eickhoff, H., Horn, M., Przewieslik, T., Theiss, D., Schneider, U., Lehrach, H., and Gobom, J. (2001) *Electrophoresis* **22,** 2844–2855
19. Gobom, J., Mueller, M., Egelhofer, V., Theiss, D., Lehrach, H., and Nordhoff, E. (2002) *Anal. Chem.* **74,** 3915–3923
20. Waetzig, G. H., Seegert, D., Rosenstiel, P., Nikolaus, S., and Schreiber, S. (2002) *J. Immunol.* **168,** 5342–5351
21. Wood, D. D., and Staruch, M. J. (1981) *Int. J. Immunopharmacol.* **3,** 31–44
22. Nagao, S., Ikegami, S., and Tanaka, A. (1984) *Cell. Immunol.* **89,** 427–438
23. Moras, M. L., Phillips, N. C., Bahr, G. M., and Chedid, L. (1985) *Int. J. Immunopharmacol.* **7,** 515–524
24. Dziarski, R. (1988) *Cell. Immunol.* **111,** 10–27
25. Jin, D. Y., Chae, H. Z., Rhee, S. G., and Jeang, K. T. (1997) *J. Biol. Chem.* **272,** 30952–30961
26. Tanabe, T., Chamaillard, M., Ogura, Y., Zhu, L., Qiu, S., Masumoto, J., Ghosh, P., Moran, A., Predergast, M. M., Tromp, G., Williams, C. J., Inohara, N., and Nunez, G. (2004) *EMBO J.* **23,** 1587–1597
27. Chamaillard, M., Philpott, D., Girardin, S. E., Zouali, H., Lesage, S., Chareyre, F., Bui, T. H., Giovannini, M., Zaehringer, U., Penard-Lacronique, V., Sansonetti, P. J., Hugot, J. P., and Thomas, G. (2003) *Proc. Natl. Acad. Sci. U. S. A.* **100,** 3455–3460
28. Uehara, A., Yang, S., Fujimoto, Y., Fukase, K., Kusumoto, S., Shibata, K., Sugawara, S., and Takada, H. (2005) *Cell. Microbiol.* **7,** 53–61
29. Till, A., Rosenstiel, P., Krippner-Heidenreich, A., Mascheretti-Croucher, S., Croucher, P. J., Schafer, H., Scheurich, P., Seegert, D., and Schreiber, S. (2005) *J. Biol. Chem.* **280,** 5994–6004
30. Ceulemans, H., Van Eynde, A., Perez-Callejon, E., Beullens, M., Stalmans, W., and Bollen, M. (1999) *Eur. J. Biochem.* **262,** 36–42
31. Sasahara, Y., Rachid, R., Byrne, M. J., de la Fuente, M. A., Abraham, R. T., Ramesh, N., and Geha, R. S. (2002) *Mol. Cell* **10,** 1269–1281
32. Oda, T., Heaney, C., Hagopian, J. R., Okuda, K., Griffin, J. D., and Druker, B. J. (1994) *J. Biol. Chem.* **269,** 22925–22928
33. Tenhoeve, J., Kaartinen, V., Fioretos, T., Haataja, L., Voncken, J. W., Heisterkamp, N., and Groffen, J. (1994) *Cancer Res.* **54,** 2563–2567
34. Tenhoeve, J., Morris, C., Heisterkamp, N., and Groffen, J. (1993) *Oncogene* **8,** 2469–2474
35. Nishihara, H., Maeda, M., Oda, A., Tsuda, M., Sawa, H., Nagashima, K., and Tanaka, S. (2002) *Blood* **100,** 3968–3974
36. Fish, E. N., Uddin, S., Korkmaz, M., Majchrzak, B., Druker, B. J., and Platanias, L. C. (1999) *J. Biol. Chem.* **274,** 571–573
37. Lekmine, F., Sassano, A., Uddin, S., Majchrzak, B., Miura, O., Druker, B. J., Fish, E. N., Imamoto, A., and Platanias, L. C. (2002) *Biochem. Biophys. Res. Commun.* **291,** 744–750
38. Popanda, O., Fox, G., and Thielmann, H. W. (1998) *Biochim. Biophys. Acta* **1397,** 102–117
39. Vishwanatha, J. K., Jindal, H. K., and Davis, R. G. (1992) *J. Cell Sci.* **101,** 25–34
40. Lay, A. J., Jiang, X. M., Kisker, O., Flynn, E., Underwood, A., Condron, R., and Hogg, P. J. (2000) *Nature* **408,** 869–873
41. Shau, H., Gupta, R. K., and Golub, S. H. (1993) *Cell. Immunol.* **147,** 1–11
42. Shau, H., Butterfield, L. H., Chiu, R., and Kim, A. (1994) *Immunogenetics* **40,** 129–134
43. Geiben-Lynn, R., Kursar, M., Brown, N. V., Addo, M. M., Shau, H., Lieberman, J., Luster, A. D., and Walker, B. D. (2003) *J. Biol. Chem.* **278,** 1569–1574
44. Shau, H., Kim, A. T., Hedrick, C. C., Lusis, A. J., Tompkins, C., Finney, R., Leung, D. W., and Paglia, D. E. (1997) *Free Radic. Biol. Med.* **22,** 497–507
45. Choi, M. H., Lee, I. K., Kim, G. W., Kim, B. U., Han, Y. H., Yu, D. Y., Park, H. S., Kim, K. Y., Lee, J. S., Choi, C., Bae, Y. S., Lee, B. I., Rhee, S. G., and Kang, S. W. (2005) *Nature* **435,** 347–353
46. Homer, C., Knight, D. A., Hananeia, L., Sheard, P., Risk, J., Lasham, A., Royds, J. A., and Braithwaite, A. W. (2005) *Oncogene* **24,** 8314–8325
47. Lasham, A., Moloney, S., Hale, T., Homer, C., Zhang, Y. F., Murison, J. G., Braithwaite, A. W., and Watson, J. (2003) *J. Biol. Chem.* **278,** 35516–35523
48. Zhang, Y. F., Homer, C., Edwards, S. J., Hananeia, L., Lasham, A., Royds, J., Sheard, P., and Braithwaite, A. W. (2003) *Oncogene* **22,** 2782–2794
49. Yokota, S., Yamamoto, Y., Shimizu, K., Momoi, H., Kamikawa, T., Yamaoka, Y., Yanagi, H., Yura, T., and Kubota, H. (2001) *Cell Stress Chaperones* **6,** 345–350
50. Won, K. A., Schumacher, R. J., Farr, G. W., Horwich, A. L., and Reed, S. I. (1998) *Mol. Cell. Biol.* **18,** 7584–7589
51. Honore, B., Leffers, H., Madsen, P., and Celis, J. (1993) *Eur. J. Biochem.* **218,** 421–430
52. Martinon, F., Agostini, L., Meylan, E., and Tschopp, J. (2004) *Curr. Biol.* **14,** 1929–1934
53. Chen, D., Duggan, C., Reden, T. B., Kooragayala, L. M., Texada, D. E., and Langford, M. P. (2004) *Biochemistry* **43,** 11796–11801
54. Chen, D., Texada, D. E., Duggan, C., Liang, C., Reden, T. B., Kooragayala, L. M., and Langford, M. P. (2005) *J. Biol. Chem.* **280,** 22425–22436
55. Liu, X. W., Lu, F. G., Zhang, G. S., Wu, X. P., You, Y., Ouyang, C. H., and Yang, D. Y. (2004) *World J. Gastroenterol.* **10,** 2701–2705
56. Deiss, L. P., Galinka, H., Berissi, H., Cohen, O., and Kimchi, A. (1996) *EMBO J.* **15,** 3861–3870
57. Maeda, S., Hsu, L. C., Liu, H., Bankston, L. A., Iimura, M., Kagnoff, M. F., Eckmann, L., and Karin, M. (2005) *Science* **307,** 734–738
58. Li, J., Moran, T., Swanson, E., Julian, C., Harris, J., Bonen, D. K., Hedl, M., Nicolae, D. L., Abraham, C., and Cho, J. H. (2004) *Hum. Mol. Genet.* **13,** 1715–1725
59. Wehkamp, J., Harder, J., Weichenthal, M., Schwab, M., Schaffeler, E., Schlee, M., Herrlinger, K. R., Stallmach, A., Noack, F., Fritz, P., Schroder, J. M., Bevins, C. L., Fellermann, K., and Stange, E. F. (2004) *Gut* **53,** 1658–1664
60. Lewis, T. S., Hunt, J. B., Aveline, L. D., Jonscher, K. R., Louie, D. F., Yeh, J. M., Nahreini, T. S., Resing, K. A., and Ahn, N. G. (2000) *Mol. Cell* **6,** 1343–1354
61. Gadgil, H. S., Pabst, K. M., Giorgianni, F., Umstot, E. S., Desiderio, D. M., Beranova-Giorgianni, S., Gerling, I. C., and Pabst, M. J. (2003) *Proteomics* **3,** 1767–1780
62. Klangby, U., Okan, I., Magnusson, K. P., Wendland, M., Lind, P., and Wiman, K. G. (1998) *Blood* **91,** 1680–1687
63. Gonzalgo, M. L., Hayashida, T., Bender, C. M., Pao, M. M., Tsai, Y. C., Gonzales, F. A., Nguyen, H. D., Nguyen, T. T., and Jones, P. A. (1998) *Cancer Res.* **58,** 1245–1252
64. Issa, J. P., Ahuja, N., Toyota, M., Bronner, M. P., and Brentnall, T. A. (2001) *Cancer Res.* **61,** 3573–3577
65. Kohonen-Corish, M. R., Daniel, J. J., te Riele, H., Buffinton, G. D., and Dahlstrom, J. E. (2002) *Cancer Res.* **62,** 2092–2097
66. Hocke, M., Richter, L., Bosseckert, H., and Eitner, K. (1999) *Hepatogastroenterology* **46,** 2333–2337
67. Kald, B., Smedh, K., Olaison, G., Sjodahl, R., and Tagesson, C. (1996) *Digestion* **57,** 472–477
68. Mannick, E. E., Bonomolo, J. C., Horswell, R., Lentz, J. J., Serrano, M. S., Zapata-Velandia, A., Gastanaduy, M., Himel, J. L., Rose, S. L., Udall, J. N., Hornick, C. A., and Liu, Z. Y. (2004) *Clin. Immunol.* **112,** 247–257